Nanotechnology **23** (2012) 015703 (7pp) doi:10.1088/0957-4484/23/1/015703

Sharp burnout failure observed in high current-carrying double-walled carbon nanotube fibers

Li Song[1,2], Geza Toth[3], Jinquan Wei[4], Zheng Liu[1], Wei Gao[1], Lijie Ci[1], Robert Vajtai[1], Morinobu Endo[2] and Pulickel M Ajayan[1,2]

[1] Department of Mechanical Engineering and Materials Science, Rice University, Houston, TX 77005, USA
[2] Research Center for Exotic Nanocarbons, Faculty of Engineering, Shinshu University, Nagano 280-8553, Japan
[3] Microelectronics and Materials Physics Laboratories, Department of Electrical and Information Engineering, EMPART Research Group, University of Oulu, PO Box 4500, FIN-90014, Finland
[4] Department of Mechanical Engineering, Tsinghua University, Beijing 100084, People's Republic of China

E-mail: ls17@shinshu-u.ac.jp and ajayan@rice.edu

Received 23 August 2011, in final form 20 October 2011
Published 8 December 2011
Online at stacks.iop.org/Nano/23/015703

Abstract
We report on the current-carrying capability and the high-current-induced thermal burnout failure modes of 5–20 μm diameter double-walled carbon nanotube (DWNT) fibers made by an improved dry-spinning method. It is found that the electrical conductivity and maximum current-carrying capability for these DWNT fibers can reach up to 5.9×10^5 S m^{-1} and over 1×10^5 A cm^{-2} in air. In comparison, we observed that standard carbon fiber tended to be oxidized and burnt out into cheese-like morphology when the maximum current was reached, while DWNT fiber showed a much slower breakdown behavior due to the gradual burnout in individual nanotubes. The electron microscopy observations further confirmed that the failure process of DWNT fibers occurs at localized positions, and while the individual nanotubes burn they also get aligned due to local high temperature and electrostatic field. In addition a finite element model was constructed to gain better understanding of the failure behavior of DWNT fibers.

S Online supplementary data available from stacks.iop.org/Nano/23/015703/mmedia

(Some figures may appear in colour only in the online journal)

1. Introduction

In the last two decades, carbon nanotubes (CNTs) have received great attention due to their outstanding electrical properties such as ballistic electronic conduction [1], high current densities and applications such as transparent conductors [2–4]. Macroscopic fibers composed of such CNTs were expected to not only yield great advances in forming high strength, lightweight, thermally and electrically conducting materials, but also to act as the building block of advanced composite materials. Many reports have been focused on preparing such CNT fibers by direct synthesis, liquid state wet-spinning and solid state dry-spinning techniques [5–16]. In the dry-spinning process, CNT fibers with diameter range of 10–500 μm were directly pulled out from continuous CNT cotton or yarn [6–12]. In the wet-spinning process, CNT powder was dispersed into solvents with polymers and then glued together into fibers of typical diameters of 20–200 μm [13–15]. Recently, CNT fibrils with diameters smaller than 1 μm have been reported by using a dielectrophoretic technique [16]. In spite of excellent electrical properties of

individual nanotubes, various types of defects such as the structural defects, or impurities and semiconducting CNTs present in the assembled CNT fibers significantly reduce the electrical conductivity and current-carrying capability. Therefore, it is important to seek alternative and/or improved methods for macroscopic fiber formation, which could retain a significant portion of the extraordinary mechanical and electrical properties of individual CNTs and in turn provide a low cost, sustainable stepping stone for future electric wire development. Meantime, it is also very important for the scientific community to understand how CNT-based fiber will behave in high current-carrying applications with the goal of one day replacing heavy traditional metallic wires. Therefore, the electric conduction of CNT-based fibers, especially the breakdown at high temperature induced by high current and Joule heating, should be investigated.

Double-walled carbon nanotube, consisting of two concentric graphene layers, has unique mechanical properties and excellent chemical stability [17–19]. DWNT is a reasonable compromise between the excellent electronic properties of single-walled nanotubes and the mechanical and chemical stability of multi-walled nanotubes. In our previous work, DWNT cottons have been mass-produced by a floating chemical vapor deposition method [20, 21]. Here, we further optimized the formerly used drawing–drying process to fabricate fibers with smaller diameters. By adding acetone to shrink the as-drawn fiber, we found that the DWNT fibers can be produced to a length of several millimeters and diameters in the range of 5–20 μm when desired. The electrical measurements revealed that DWNT fibers exhibit high electrical conductivity and excellent current-carrying capability, suggesting their potential applications in lightweight electrical cables. Moreover, the DWNT fibers pose a unique electrical breakdown behavior under high current load. We believe that this study will provide important insights into the stability and failure properties of carbon nanotube-based fibers for electronics applications.

2. Experimental section

The cotton-like DWNT samples were prepared by a floating catalyst CVD method using xylene and ferrocene as the carbon and catalyst source at the temperature of 1000 °C. Two-step purification processes, including oxidation at 350 °C for 24 h and subsequent immersion in 37 wt% HCl solution for two days, were carried out to remove amorphous carbon and iron catalyst particles from the DWNTs samples. A custom-made fiber spinning setup was used to draw out the DWNT cottons into a fiber, as shown in figure 1 [21]. We used a sharp curved hook to draw a very small strand from the purified DWNT samples. Several drops of acetone were than introduced into the initial strand in order to enhance its stiffness for future fiber pulling. During the pulling–winding process, acetone solution was continuously dropped onto the as-spun fibers. A hot air blower was used to enhance the drying of the as-drawn fibers. It was found that the quick evaporation of acetone could efficiently shrink and compact the nanotubes inside the fiber, thus producing fibers with much smaller diameters compared

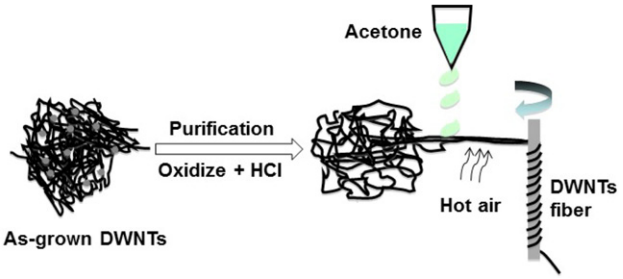

Figure 1. Schematics of the fabrication process of DWNT fibers.

to our previous work [20, 21]. It is found that centimeter-long DWNT fibers with diameters of 5–20 μm could be continuously drawn from our purified nanotubes.

The measurements of electrical conductivity and current-carrying capability were performed on the DWNTs fibers with different diameters. The centimeter-long DWNT fibers were first bonded on a silicon–silicon oxide wafer by several silver electrodes with different gaps. Their electrical conductivities were tested by measuring the I–V characteristics in air with the four-probe configuration through a Keithley electrometer with a custom-made test-program. The current-carrying capability experiments were performed by continuously increasing the bias voltage on the fibers using a two-probe arrangement. The diameter of the tested fiber was measured by SEM. For the subsequent calculations the fiber cross-section was assumed to be circular and uniform along the fibril axis.

Scanning electron microscopy (JEOL 6500), Raman spectroscopy (RENISHAW InVia), transmission electron microscopy (JOEL 2010), and thermal gravimetric analysis (TGA, Thermo Plus-TG8120) were used for fiber's characterization.

3. Results and discussions

3.1. The morphology of DWNT fibers

Figure 2(a) shows the low-magnification scanning electron microcopy (SEM) image of a typical as-drawn DWNT fiber. It is clearly seen that the fiber shows uniform diameter along the entire length. The diameter of the as-spun DWNT fiber is controllable in the range of 5–20 μm, which is much smaller than previously reported. This is due to the shrinking and compacting of the fibers from the quick evaporation of acetone injected during drawing [21, 22]. Figure 2(b) reveals that most of the nanotube bundles inside the microfiber are entangled but also show a smooth surface along the fiber axis. Figure 2(c) is a typical transmission electron microscopy (TEM) image of DWNT fibers. It shows that most of nanotubes inside the fiber are DWNTs with diameters of 1–2 nm. The sectional TEM image (the inset of figure 2(c)) indicates the hexagonal-close-packed structure of nanotubes inside DWNT bundles. Polarized Raman spectroscopy was performed on the as-drawn fiber for detecting the nanotube orientation inside the fiber. Figure 2(d) shows the Raman intensity change as a function of the angle between the sample axis and the optical polarization axis. The intensity of Raman G and D modes for

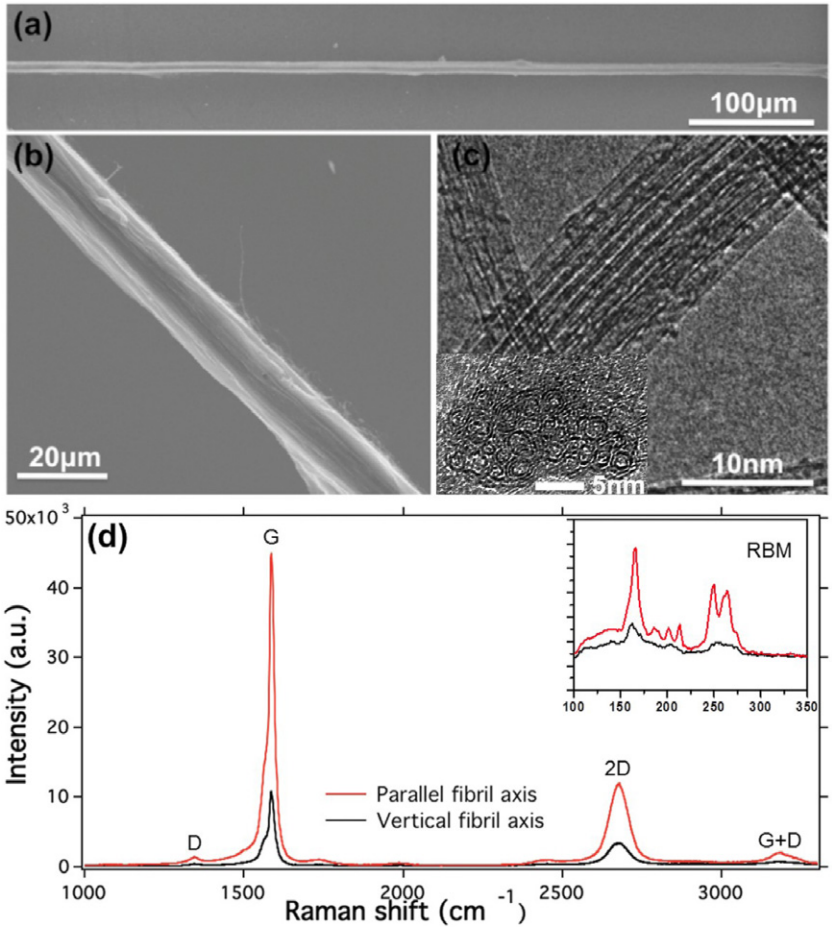

Figure 2. (a) Low-magnification SEM image of a DWNT fiber with uniform diameter of ∼15 μm. (b) The SEM image indicates a smooth surface of the DWNT fiber. (c) High-resolution TEM image, taken from the trunk of a bundle inside a DWNT fiber. The inset is a sectional TEM image of a DWNT bundle. (d) Polarized Raman spectra collected from a DWNT fiber. Spectra are recorded with the analyzer axis parallel to the polarization axis of the 514.5 nm excitation laser. The inset spectrum indicates the polarized Raman breathing-mode peak of DWNTs.

the case of the fiber axis parallel to the optical polarization direction are approximately four times higher than that of the fiber axis vertical to the optical polarization direction. This indicates the nanotubes have been drawn out strongly orientated along the fiber axis, which is in agreement with the SEM and TEM observations. The inset of figure 2(d) shows the radial breathing vibration mode (RBM) of DWNTs in the low-frequency 100–300 cm^{-1} region, which is very sensitive to the diameter of individual nanotubes inside the fibers. There are two resonant Raman peaks in the RBM regions. Considering DWNT has two concentric graphene layers, the two resonant peaks could be assigned to the inner tube and the outer tube of DWNTs. According to the relation between diameter and frequency ($\omega_{RBM} = 224/d + 14$ (nm)) [3, 23], it is calculated that the DWNTs inside the drawn fibers have inner diameters of 0.8–1 nm and outer diameters of 1.4–1.6 nm, which is consistent with our above TEM observation.

3.2. The electrical measurement of DWNT fibers

The electrical conductivity and current-carrying capability of DWNT fibers with different diameters were measured by a four-probe configuration in air. Figure 3(a) shows an optical image of a DWNT fiber contacted with several metal (Ag) electrodes. A typical I–V curve of a DWNT fiber is shown in figure 3(b). Considering the similarities in the microstructure, the material's properties and the applicability, we have selected a commercial polyacrylonitrile (PAN) carbon fiber as a reference. The linear behavior of the curves at large bias voltage range in our measurements and the similarity of the two-probe and four-probe measurements indicate good ohmic contacts between the fibers and the electrodes. The conductivity of DWNT fiber is calculated as 3.1×10^5 S m^{-1}, which is over ten times higher than that of PAN carbon fiber (2.2×10^4 S m^{-1}). It is worth mentioning that it is still two orders of magnitude lower than that of current copper wire with similar diameter. The electric conductivity experiments were repeated with several samples of different diameters. We found that the conductivity of the as-drawn DWNT fibers ranged from 0.9×10^4 to 5.9×10^5 S m^{-1}, where smaller diameter fibers exhibited higher conductivity values.

The current-carrying capability of DWNT fibers was investigated in air by continuously increasing the bias voltage loaded on the fiber with two electrodes. Figure 3(c) shows an

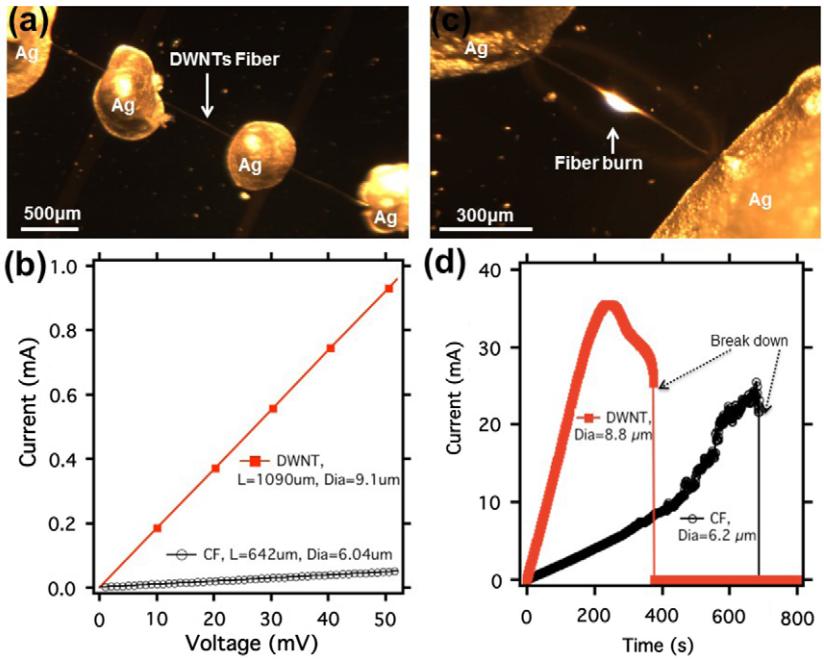

Figure 3. (a) An optical image of a DWNT fiber device with four-probe electrodes. (b) Typical I–V characteristics of a DWNT fiber with diameter of 9.1 μm and a PAN carbon fiber with diameter of 6.04 μm. (c) An optical image of a burning DWNT fiber when high current is flowing. (d) Typical current-carrying capabilities of a DWNT fiber and a PAN carbon fiber in air. The load current was increased continuously by increasing the bias voltage at the rate of 0.2 mV/step.

optical image of a burning DWNT fiber when passing a high current. It is found that most of the fibers failed in the middle of the contacted segments. The current-carrying capabilities for a DWNT fiber and a PAN carbon fiber are shown in figure 3(d). It can be seen that the current suddenly burns the PAN carbon fiber when the value reaches its maximum at 25.5 mA. The as-drawn DWNT fibers, however, exhibit a unique, more favorable burning process when the possible application for electrical wiring is considered. Here the sudden, catastrophic failure is not desired since the cable prefers to withstand the sudden and short current bursts close to their tolerance limit. The current first reaches a maximum value of 35.4 mA, then continuously reduces down to 24.4 mA with loaded bias voltage increasing, and suddenly falls to 0 mA when the fiber burns and breaks. A video of the burning process is shown in the supporting material (available at stacks.iop.org/Nano/23/015703/mmedia). It is visible that the middle part of the DWNTs' fiber section first becomes very hot (glowing red in the video) due to high local temperature induced by high current flow, and then breaks down by nanotubes burning away at the center region of the fiber (also see figure 3(c)). We suggest that the individual nanotubes and bundles inside the DWNT fiber start to fuse and burn when the local electrical field becomes high, thus the increased resistance, as shown in the supporting video (available at stacks.iop.org/Nano/23/015703/mmedia) and the breakdown point of figure 3(d). There were some cases when the fiber failure occurred further away from the center point. This can be explained with the irregularities in the width of the fiber or other imperfections introduced during manufacturing. In order to get the average value, the current-carrying capability experiments were also repeated in different sections of the same fiber. It is found that the maximum current value ranged from 30 to 100 mA (the range is due to the diameter differences of the DWNT fibers). Table 1 shows the electrical conductivity and current-carrying capability results obtained from DWNT fibers with different diameters. It is estimated from table 1 that the maximum current density for DWNT fiber with the smallest diameter could reach as high as 1.03×10^5 A cm^{-2}, which is superior to the PAN carbon fiber (8×10^4 A cm^{-2}). We note that this value represents a value where the lower limit as the cross-section used in the calculation is the geometrical cross-section of the fiber whereas the actual cross-section carrying the current is much smaller as the fiber is only loosely packed with the nanotubes. With the free volume of the fiber considered, its effective cross-sectional area needs to be determined to obtain the real modulus [24–26]. From SEM images of the broken tip of fibers, we can assume the nanotube bundles have a similar diameter (100 nm) and interstitial spacing (100 nm). The percentage free of the volume is calculated by using the $(V_f/V) = 1 - [\pi(D)^2/4d^2]$, where D is the diameter of nanotube bundles, d is the distance between two bundles. The approximate free volume is 80% ± 10% for DWNT fibers. Furthermore, considering the interstitial space between the single nanotubes in each bundle, the percentage of the free volume is calculated to be 10% ± 5% provided that the DWNTs are in hexagonal-close-packed structure within the bundle [27, 28]. From these assumptions, the percentage of the effective cross-sectional area is calculated to be 15% ± 10%. Therefore, the current density for DWNT fiber could reach as high as 7×10^5 A cm^{-2}, in the case of a nearly perfect fiber.

Table 1. The comparison of electrical conductivity and current-carrying capability of DWNT fibers with different diameters and PAN carbon fiber. The lengths of tested fibers were around 500 μm.

	Sample					
Data	DWNT fibril#1	DWNT fibril#2	DWNT fibril#3	DWNT fibril#4	DWNT fibril#5	Carbon fiber
Diameter (μm)	5.6	8.8	9.1	13.3	17.6	6.1
Conductivity (S m^{-1})	5.9×10^5	3.8×10^5	3.1×10^5	1.3×10^5	9.3×10^4	2.2×10^4
Max. current-carrying (mA)	25.6	35.4	43.2	58.5	72.1	24

3.3. The failure behavior of DWNT fibers

In order to have a better understanding of the burning failure behavior, SEM and TEM observations were performed to reveal the detailed structure of the DWNT and PAN fibers at the failure point. It is observed that disjointed parts across the length of the PAN fiber (figure 4(b)), during high current failure, have burnt off forming large holes in the fiber with a morphology resembling a Swiss cheese. Some parts of the material seem to have been removed from the PAN fiber at different locations along the fiber. This type of failure becomes catastrophic because it makes the fiber extremely non-uniform. We suggest that this failure could be ascribed to PAN fiber's oxidization in air by locally increased temperature when the high current flows at a smaller cross-section.

In the case of DWNT fiber, the failure has occurred at a well-defined single location, as shown in figure 4(a). This failure and the broken ends can be attributed to the burning of carbon nanotubes in air induced by the high local temperature. The high magnification SEM and TEM images in figures 4(c)–(g) feature the close-up views of the broken end of a DWNT fiber of 12 μm diameter, clearly showing several protruding smaller nanotube bundles terminated in sharp and fused tips. These bundles at the broken ends of DWNT fibers are composed of aligned, compacted nanotubes tapering to a single nanotube at the tip. Some residual catalyst particles coated with amorphous carbon are observed in figure 4(e). We suggest that this morphology of the broken DWNTs fiber end occurs during the Joule-heating-induced inhomogeneous break-up events taking place in a large number of individual nanotubes that constitute the fiber [29–31]. The particular alignment of nanotubes seen at the broken ends of the DWNT fiber is most probably due to the high electric field at the location close to the instant of the fiber breakdown; similar structures were reported earlier in the case of SWNTs and MWNTs [32]. When the fiber fails the current stops flowing through the formed gap; however, the rest of the carbon nanotube fiber remains unchanged, its conductivity is still high. As a result, the applied voltage drops on the gap itself, not on the fiber, and it causes high electrostatic field. When the rest of the fiber is negatively charged the small fibrils in the fiber exert repulsive forces on each other and they move to the furthest mechanically allowed position. The process is localized to a few micrometer regions of the freshly burned tips, however this electrostatic force could open a larger part of the fiber. We assume that the opening up is localized as the inner structure of the fibers is mechanically stable in the long run, the fibrils which run independently for a few micros touch and entangle with each other.

3.4. The finite element model of fibers

To gain a better view of the burnout behavior, the localized temperature fields and the electrical conduction in PAN and DWNT fibers, a finite element model was constructed using the Ansys software package. In this model, DWNT and PAN fibers are considered as a core–shell material. This is due to the strong anisotropy in the electrical conductivity as described by others [33, 34]. According to the simulation results the core–shell structure describes the electrical conductance and the Joule heating better than applying the anisotropic materials properties only. It might be due to the fact that the electrical contact is on the surface of the fibers only, thus most current will flow on the outer part of the fiber. Thermal conductivity for carbon fiber (70 W m^{-1} K^{-1}) was taken from the references of Amoco Performance Products, Inc. Thermal conductivity of DWNT (100 W m^{-1} K^{-1}) was estimated by using the results of Hsu *et al* [35]. The applied load on the electrical contacts was 3.76 V and 6.88 V for DWNT and PAN fibers respectively. These voltage values correspond to the measured peak currents in DWNT and PAN fibers, which were followed by the electrical breakdown and burning. Our simulated results—shown in figures 5(c) and (d)—reveal that the fiber will have a burnout failure at the center region when the temperature increases to a higher value than the oxidation temperature of the material. This has been confirmed by experimental observations. At the failure region, the calculated local temperature for PAN and DWNT fibers is consistent with the above TGA data, hence the core–shell structure adequately describes the electrical conductivity and the Joule heating in both systems. See the detailed finite element simulation in S1 (available at stacks.iop.org/Nano/23/015703/mmedia).

4. Conclusions

We have fabricated DWNT fibers with diameters in the range of 5–20 μm by an optimized drawing method. Electrical measurements revealed that the conductivity of DWNT fibers is over an order of magnitude higher than that of commercial PAN-based carbon fibers. The high current-carrying capability of the DWNT fibers and their failure features upon electric burning were studied. It is found that the current-carrying

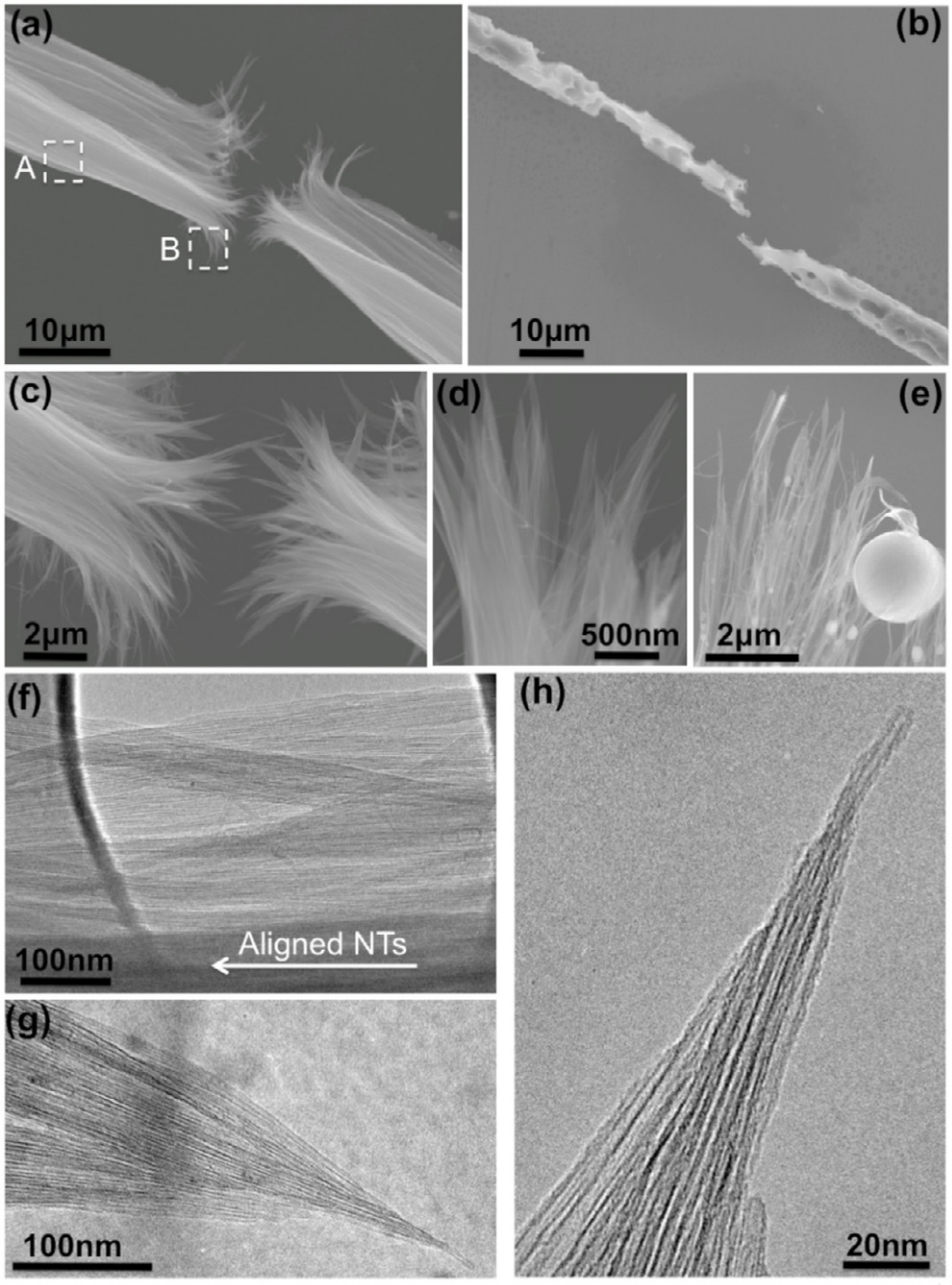

Figure 4. (a), (b) SEM images of the broken point for a DWNT fiber and a PAN carbon fiber. (c)–(e) High magnification SEM images of the broken DWNT fiber ends, showing the two ends consist of many cone-like tips separated by few micros gap. (f), (g) TEM images of the trunk part and the broken ends for a DWNT fiber. (h) High magnification TEM image of a broken end of DWNT fiber, revealing that the conical tips are generally composed of well-aligned and firmly compacted nanotubes with a single nanotube burning-opened tip.

capability of DWNT fibers can reach as high as 10^5 A cm^{-2}, which is one order higher than standard carbon fiber. Moreover, the high current quickly oxidizes and burns PAN fiber with cheese-like morphology when the maximum current is reached, causing violent and harmful material ejection over the entire length of the fibers, while DWNT fibers show a much slower breakdown behavior due to the slow burning process in the fiber. SEM and TEM observations prove that the failure of DWNT fiber occurs at single localized positions and the individual nanotubes get burnt out and are aligned due to localized temperature rise. These investigations allow us to better understand the breakdown failure behaviors of carbon-based fibers under high current and thus point out the direction for the future development of carbon nanotube-based electric wiring.

Acknowledgments

This work is supported by the Air Force Research laboratories under contract FA8650-05-D-5807. We acknowledge the additional financial support from Exotic Nanocarbons, Japan Regional Innovation Strategy Program by Excellence, JST and

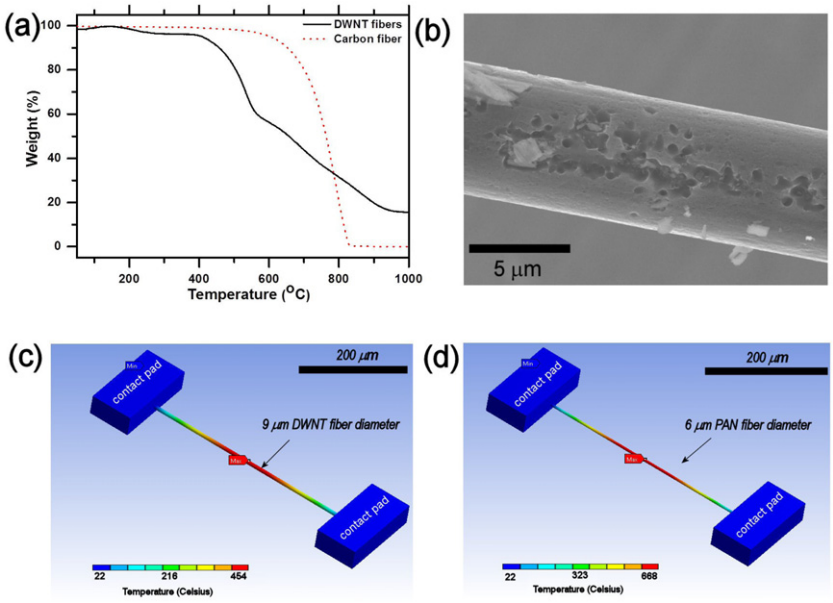

Figure 5. (a) TGA of the DWNT and PAN fibers; (b) SEM image of PAN carbon fiber after quick oxidization in air; (c) and (d) simulated thermal field for structural effect maximum temperature investigations for DWNT and PAN fibers.

Green Innovation Project from Shinshu University. Dr Toth was supported by the Academy of Finland project 128908 and EC FP7 project 228539

References

[1] Javey A, Guo J, Wang W, Lundstrom M and Dai H J 2003 *Nature* **424** 654
[2] Baughman R H, Zakhidov A A and de Heer W A 2002 *Science* **297** 787
[3] Saito R and Dresselhaus M S 1998 *Physical Properties of Carbon Nanotubes* (London: Imperical College Press)
[4] Yao Z, Kane C L and Dekker C 2000 *Phys. Rev. Lett.* **84** 2941
[5] Behabtu N, Green M J and Pasquali M 2008 *Nano Today* **3** 24
[6] Li Y L, Kinloch I A and Windle A H 2004 *Science* **304** 276
[7] Jiang K L, Li Q Q and Fan S S 2002 *Nature* **419** 802
[8] Zhang M, Atkinson K R and Baughman R H 2004 *Science* **306** 1358
[9] Zhang X F, Li Q W, Tu Y, Li Y, Coulter J Y, Zheng L X, Zhao Y H, Jia Q X, Peterson D E and Zhu Y T 2007 *Small* **3** 244
[10] Koziol K, Vilatela J, Moisala A, Motta M, Cunniff P, Sennett M and Windle A H 2007 *Science* **318** 1892
[11] Zhang X F *et al* 2007 *Adv. Mater.* **19** 4198
[12] Zhong X H, Li Y L, Liu Y K, Qiao X H, Feng Y, Liang J, Jin J, Zhu L, Hou F and Li J Y 2010 *Adv. Mater.* **22** 269
[13] Vigolo B, Penicaud A, Coulon C, Sauder C, Pailler R, Journet C, Bernier P and Poulin P 2000 *Science* **290** 1331
[14] Ericson L M *et al* 2004 *Science* **305** 1447
[15] Jang E Y, Kang T J, Im H, Baek S J, Kim S, Jeong D H, Park Y W and Kim Y H 2009 *Adv. Mater.* **21** 4357
[16] Ma J, Tang J, Zhang H, Shinya N and Qin L C 2009 *ACS Nano* **3** 3679
[17] Saito R, Dresselhaus G and Dresselhaus M S 1993 *J. Appl. Phys.* **73** 494
[18] Tanaka K, Aoki H, Ago H, Yamabe Y and Okahaka K 1997 *Carbon* **35** 121
[19] Endo M, Muramatsu H, Hayashi T, Kim Y A, Terrones M and Dresselhaus M S 2005 *Nature* **433** 476
[20] Wei J Q, Jiang B, Wu D H and Wei B Q 2004 *J. Phys. Chem.* B **108** 8844
[21] Ci L J, Punbusayakul N, Wei J Q, Vajtai R, Talapatra S and Ajayan P M 2007 *Adv. Mater.* **19** 1719
[22] Chakrapani N, Wei B Q, Carrillo A, Ajayan P M and Kane R S 2004 *Proc. Natl Acad. Sci.* **101** 4009
[23] Rao A M, Chen J, Richter E, Schlecht U, Eklund P C, Haddon R C, Venkateswaran U D, Won Y K and Tomanek D 2001 *Phys. Rev. Lett.* **86** 3895
[24] Zuo J M, Vartanyants I, Gao M, Zhang R and Nagahara L A 2003 *Science* **300** 1419
[25] Coleman J N, Blau W J, Dalton A B, Munoz E, Collins S, Kim B G, Razal J, Selvidge M, Vieiro G and Baughman R H 2003 *Appl. Phys. Lett.* **82** 1682
[26] Pan Z W, Xie S S, Lu L, Chang B H, Sun L F, Zhou W Y, Wang G and Zhang D L 1999 *Appl. Phys. Lett.* **74** 3152
[27] Thess A *et al* 1996 *Science* **273** 483
[28] Dresselhaus M S, Dresselhaus G and Saito R 1995 *Carbon* **33** 883
[29] Huang J Y, Chen S, Jo S H, Wang Z, Han D X, Chen G, Dresselhaus M S and Ren Z F 2005 *Phys. Rev. Lett.* **94** 236802
[30] Huang J Y, Chen S, Wang Z Q, Kempa K, Wang Y M, Jo S H, Chen G, Dresselhaus M S and Ren Z F 2006 *Nature* **439** 281
[31] Moon S *et al* 2007 *Nanotechnology* **18** 235201
[32] Wei Y, Jiang K L, Liu L, Chen Z and Fan S S 2007 *Nano Lett.* **7** 3792
[33] Zhou Z, Lai C, Zhang L, Qian Y, Hou H, Reneker D H and Fong H 2009 *Polymer* **50** 2999
[34] Lina C-T, Leea C-Y, Chinc T-S, Xiangd R, Ishikawae K, Shiomie J and Maruyama S 2011 *Carbon* **49** 1446
[35] Hsu I-K, Pettes M T, Bushmaker A, Aykol M, Shi L and Cronin S B 2009 *Nano Lett.* **9** 590